

Ga₂O₃/HZSM-5 Propane Aromatization Catalysts: Formation of Active Centers via Solid-State Reaction

GEOFFREY L. PRICE*¹ AND VLADISLAV KANAZIREV†

*Department of Chemical Engineering, Louisiana State University, Baton Rouge, Louisiana 70803, and
†Institute of Organic Chemistry, Bulgarian Academy of Sciences, 1040 Sofia, Bulgaria

Received March 3, 1990; revised May 30, 1990

An active and very selective catalyst for propane conversion to aromatics near atmospheric pressure and 750–850 K is formed by ball-milling 2–10 wt% Ga as Ga₂O₃ with HZSM-5 followed by hydrogen reduction at about 850 K for 2 h. Microbalance TPR experiments and X-ray diffraction studies along with catalytic testing have helped establish that the intimate physical mixture of Ga₂O₃ with HZSM-5, the acidity of the zeolite, and the hydrogen reduction are all necessary to generate the highly active form of the catalyst. The active species is probably Ga(I) as a zeolitic cation and is not incorporated in the zeolite lattice. © 1990 Academic Press, Inc.

INTRODUCTION

Ga-containing zeolites for light paraffin aromatization have received considerable interest since their incorporation in the Cyclar (1) process. Many different formulations of Ga/HZSM-5 have been found to be useful for paraffin aromatization including catalysts prepared by ion exchange (2) or impregnation (3) of gallium salts with ZSM-5, gallosilicates (4), and mechanical mixtures of Ga₂O₃ with ZSM-5 (5).

We have focused on mechanical mixtures of Ga₂O₃ with HZSM-5 and have been able to produce remarkably active and selective catalysts via systematic preparation. These catalysts are superior to those reported by Gnep *et al.* (6), even though lower Ga loadings were generally used in our studies. We report here our findings on the requirements for forming an active catalyst in this system.

EXPERIMENTAL

A. Catalysts

The catalyst base was Linde ELZ-105-6 which is an experimental HZSM-5 material. The manufacturer-reported composition is

3.73% Al₂O₃, 94.95% SiO₂, and 0.03% Na₂O by weight. Gallium-containing catalysts were prepared by ball-milling β-Ga₂O₃ with the HZSM-5 base for 3 h. Three gallium catalysts containing nominally 2, 5, and 10 wt% Ga (on an elemental basis) were prepared. We refer to these catalysts as "KPD" catalysts with a numerical suffix indicating the gallium loading on an elemental basis by weight.

Other catalysts containing a silicalite base (Linde S-115, SiO₂, 99%, Al₂O₃, 0.53%; Na₂O, 0.01%) and NaX base (Linde 13X) were also prepared for comparison purposes by ball-milling β-Ga₂O₃ with the appropriate base zeolite for 3 h.

For catalytic studies, the ball-milled catalysts were pressed into 1-cm-diameter tablets at 3500 bar which were then ground and sieved to 40- to 60-mesh particles.

B. Catalytic Reactor

The catalysts were loaded in a stainless-steel tubular reactor (10-mm i.d.) and heated by a digitally controlled electric furnace. Prior to use, catalysts were pretreated either in He (60 cm³/min) or in a H₂/He mixture (130 cm³/min He and 30 cm³/min H₂) by temperature programming as follows: room temperature up to 393 K (2 K/min), hold at

¹ To whom correspondence should be addressed.

393 K for 2 h, 393 to 848 K (1 K/min), hold at 848 K for 2 h. In some cases an additional treatment with the H₂/He mixture was applied during the catalytic testing.

Matheson instrument-grade propane, containing about 250 ppm C₂H₄ and roughly 100 ppm C₃H₆, and high-purity He or He/H₂ were fed through digital flow controllers and mixed in the proper ratio before the reactor inlet. The pressure in the whole system was kept constant by means of a backpressure regulator. Heating all lines downstream from the reactor outlet and using additional He diluent in the effluent helped to prevent product condensation.

The total gas flow rate in the reactor was 130 cm³ min⁻¹ at a propane mass flow of 0.018 mol/h and WHSV of 1 h⁻¹. Experiments were conducted at a nominal total pressure of 123 kPa and propane partial pressure of 14 kPa.

C. Gas Chromatograph

Reactor products were analyzed on line with a Hewlett–Packard 5880 equipped with an FID detector, 30-m wide-bore capillary column (Supelco SPB-1), automated gas sampling valve injection, and cryogenic oven. A typical analysis is given in Table 1.

D. Microbalance

The microbalance experiments were performed in a Perkin–Elmer TGA-7 interfaced to an IBM PS/2 with a Perkin–Elmer TAC-7. Balance purge gas was 80 cm³/min of He and reagent gas was 40 cm³/min of a H₂/He mixture which could be varied in composition from 0 to 75% H₂. Both temperature-programmed and isothermal experiments were performed.

E. X-Ray Diffraction

A Scintag PAD-V X-ray diffractometer equipped with a CuK α radiation source operated at 1.6 kW and a Kevex Peltier-cooled solid-state silicon detector was used to obtain diffraction data. The system is completely automated with a Micro VAX II computer and software which allows back-

TABLE 1
Typical Chromatographic Analysis^a

Component	Weight %
Methane	1.851
Ethylene	3.368
Ethane	1.874
Propylene	4.164
Propane	78.780
i-Butane	0.151
1-Butene + i-butene	0.313
1,3-Butadiene	0.022
n-Butane	0.237
trans-2-Butene	0.031
cis-2-Butene	0.098
C ₅ ⁺ Nonaromatics ^b	0.064
Benzene	3.689
Toluene	3.512
Ethylbenzene	0.087
m- + p-Xylene	1.098
Styrene	0.023
o-Xylene	0.324
C ₉ aromatics ^c	0.167
Naphthalene	0.022
C ₁₁ ⁺ Aromatics ^d	0.024

^a KPD-10, H₂ pretreatment at 803 K, reaction temperature 803 K.

^b Primarily n- and i-pentane, components partially resolved.

^c Primarily trimethylbenzenes, components partially resolved.

^d Primarily methylnaphthalenes, components partially resolved.

ground subtraction, CuK α stripping, peak location, deconvolution, and lattice constant calculations. All reported spectra have been background corrected and CuK α stripped.

Exact angle correction was performed using a NaA zeolite external standard prepared by Charnell's recipe (7) and assigning actual reflection angles by comparison with the computed powder pattern of von Ballmoos (8).

Samples were prepared by placing approximately 20 mg of sample on a glass slide (approximately 2 × 2 cm), adding a drop of water, and smearing the sample uniformly over the slide. The samples were dried at 383 K for 2 h and placed in a desiccator over

1 M NH₄Cl solution for at least 10 h prior to the diffraction experiment. Samples prepared in this manner were compared with samples mounted via the more conventional technique of pressing the material in a 1-mm-deep planchet. Spectra of samples on glass slides showed about a 30% decline in reflection intensity and a minor amorphous background from the slide which was easily removed by background subtraction.

Two types of scans were performed. For unit cell size calculations and β -Ga₂O₃ content analysis, spectra were recorded from 3 to 60° 2 θ at 1°/min. Unit cell sizes were calculated by assigning Miller indices to the ZSM-5 bands by comparison with the computed pattern of von Ballmoos (8). For β -Ga₂O₃ content, the sum of peak heights at about 31.61° and 35.12° 2 θ (β -Ga₂O₃ lines) divided by the sum of peak heights at about 24.25° and 29.16° 2 θ (ZSM-5 lines) was taken as being proportional to Ga₂O₃/ZSM-5. These lines were selected because of their relative proximity and because they are well resolved from other bands. A calibration curve which showed good linearity was constructed from the catalysts which were prepared by ball-milling β -Ga₂O₃ with the HZSM-5, but had not been subjected to chemical conditioning. Ga₂O₃ contents of unknown samples were determined using this calibration. Also, the absolute reflection intensities of the Ga₂O₃ lines in the ball-milled (but not chemically treated) catalysts were virtually identical to the absolute reflection intensities of lines in pure β -Ga₂O₃ multiplied by the weight fraction of Ga₂O₃ in the sample. This indicates that there is no phase modification or induced reaction of Ga₂O₃ with HZSM-5 upon ball-milling.

For aluminum content calculations, scans were performed from 43 to 47° 2 θ at 0.1°/min. The method of Bibby *et al.* (9) was used to determine an Al₂O₃ content by measuring the angle difference between the ZSM-5 bands at about 45.0° and 45.5° 2 θ . To precisely compute these peak positions, bands in the 44–46° 2 θ regions were deconvoluted using the proprietary Scintag soft-

ware which minimizes the difference between the actual spectrum and a theoretical curve based upon a series of peaks with split Pearson VII profiles.

RESULTS

A. Reaction Studies

Figure 1 compares the reaction of propane over the HZSM-5 substrate with KPD-2 after 2 and 30 h on stream without any H₂ treatment. This figure demonstrates that when first put on stream, KPD-2 does not exhibit activity and selectivity much different from HZSM-5. However, a significant increase in aromatics production with a concurrent decrease in methane is evident after 30 h on stream. We have observed this trend continuing for an experiment which lasted longer than 1 week.

Hydrogen treatment can accelerate this activation process as shown in Fig. 2. The upper chart shows the product distribution obtained from a KPD-2 catalyst which was first put on propane for 30 h followed by 2 h of H₂ at 848 K and subsequently returned to propane. The product distribution is virtually identical to the distribution shown in the lower chart (Fig. 2), which depicts a KPD-2 catalyst which was treated with H₂ at 848 K for 2 h prior to any propane feed.

Figure 3 gives a comparison of the product distributions obtained using KPD-2, KPD-5, and KPD-10 with H₂ pretreatment at 848 K for 2 h. Higher Ga loadings tend to reduce the global activity but also strongly reduce the selectivity to methane concurrent with a decrease in aromatics selectivity and increase in C₄ selectivity. More details of the reaction kinetics will be presented in a forthcoming publication.

Finally, Fig. 4 gives a comparison of KPD-2, -5, and -10 at 30, 7.5, and 4.5 h on stream, respectively, with no hydrogen treatment. This figure shows that the higher the initial Ga₂O₃ loading, the faster the propane activation process proceeds. More details of this observation are provided in a previous publication (15).

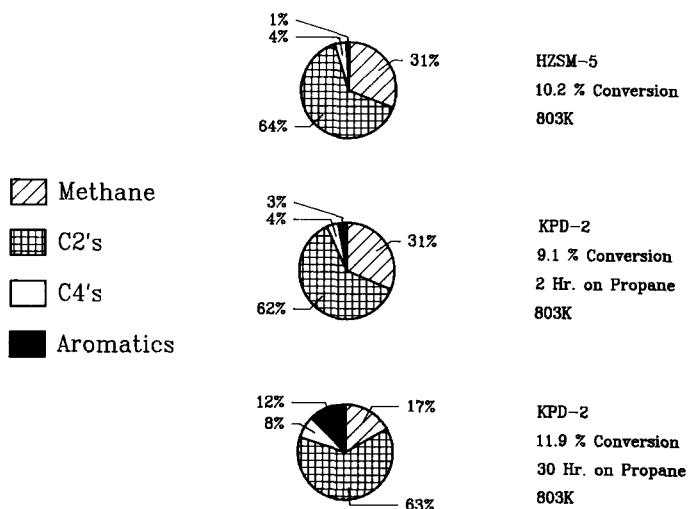


FIG. 1. Comparison of HZSM-5 with KPD-2 at 2 and 30 h on stream. Reaction temperature 803 K, no hydrogen treatment, propane reactant.

B. Microbalance Studies

Since reduction appears to be a critical process in the formation of an active catalyst, characterization of this process was performed in a microbalance. Figure 5 depicts several typical temperature-programmed reductions (TPR) which demonstrate the effect of H_2 partial pressure, programming rate, and the intimacy of the physical mixture.

Note in Fig. 5 the weight loss band at about 940 K for the sample treated at 10 K/min with $P_{H_2} = 2.5$ kPa (curve A). We have assigned this band as hydrogen reduction of Ga_2O_3 and provide the following evidence to show that it is not due to other effects such as dehydration, dehydroxylation, or other elimination processes from the Ga_2O_3 or HZSM-5. First, the band shifts to 875 K when the hydrogen partial pressure is increased to $P_{H_2} = 23$ kPa with the pro-

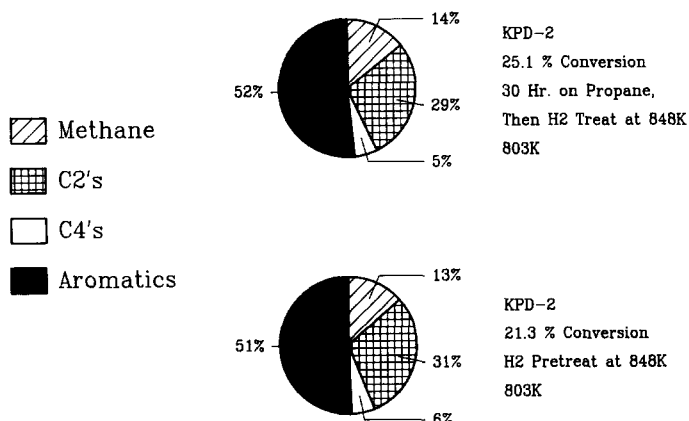


FIG. 2. Comparison of KPD-2 post-treated with hydrogen (upper chart) with KPD-2 pretreated with hydrogen (lower chart) for propane aromatization at 803 K.

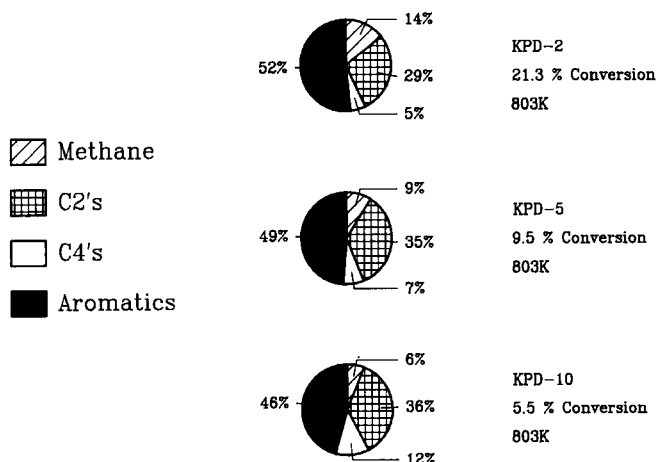


FIG. 3. Propane aromatization at 803 K for hydrogen-pretreated catalysts. Pretreatment temperature 848 K.

gramming rate held constant at 10 K/min (curve B). Second, when the programming rate is reduced to 3 K/min (holding the H₂ pressure at 23 kPa), the band shifts to about 845 K (curve D). This indicates a kinetic or diffusion-controlled process which involves hydrogen. Third, neither HZSM-5 nor Ga₂O₃ individually shows this band. In fact, β -Ga₂O₃ undergoes less than 0.2% weight reduction upon temperature programming to 1000 K in hydrogen. This suggests that

the intimate physical mixture of HZSM-5 and Ga₂O₃ is necessary for the reduction to proceed. To test this hypothesis, Ga₂O₃ and HZSM-5 were added without mixing in the microbalance pan. No reduction band was noted up to 950 K with $P_{H_2} = 23$ kPa (Fig. 5, curve C). Finally, an intimate physical mixture of Ga₂O₃ and NaX zeolite (ball-milled 3 h) did not undergo reduction in hydrogen under identical conditions. This indicates that the ball-milling process does not

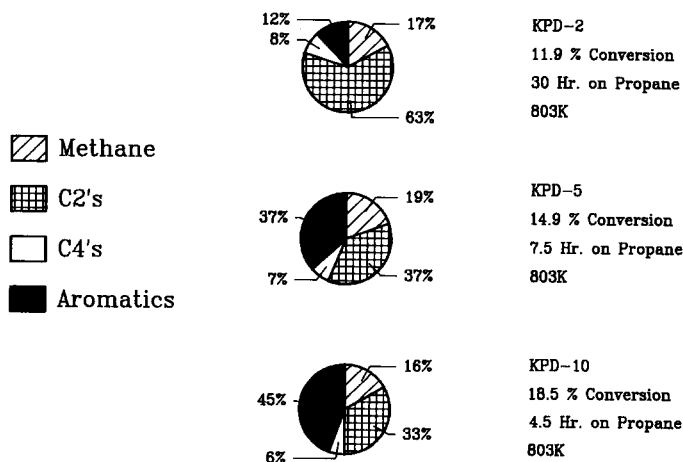


FIG. 4. Comparison of propane aromatization at 803 K for catalysts not treated with hydrogen.

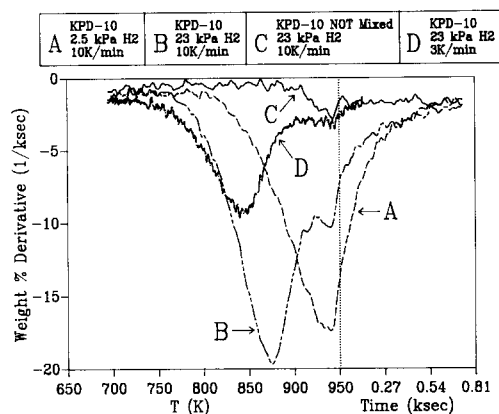


FIG. 5. Microbalance of KPD-10. Temperature programming to 950 K, then isothermal at 950 K.

inherently induce the activation of the Ga_2O_3 . Therefore, it appears that both the intimate physical mixture and the zeolite acidity are necessary before the reduction process will take place.

Isothermal microbalance experiments have been very useful in quantitative determinations of weight loss. In these experiments, the specimen is dried isothermally at 880 K in He until constant weight is achieved and then the sample is brought to reduction temperature (815, 842, or 870 K). H_2 at $P_{\text{H}_2} = 23$ kPa is then substituted for a portion of the He so that the overall purge rates in the microbalance remain constant. The reduction process is observed as a monotonic decline in specimen weight until a new stable weight is established. These results are shown in Fig. 6 and several important aspects should be noted. First, neither HZSM-5 nor Ga_2O_3 shows significant reduction when observed individually. The effect of changing temperature for the KPD-10 series is as expected; higher temperature yields higher initial rates of reduction, but the initial rate of reduction at 870 K is only marginally larger than that at 842 K. At a constant temperature of 842 K, the initial rate of reduction is $\text{KPD-10} > \text{KPD-5} > \text{KPD-2}$ which is in the same order as the rate of catalyst activation by the propane

reaction. Note also that the ultimate relative weight loss for each of the KPD-10 samples is roughly the same. The KPD-5 sample shows an ultimate relative weight loss near, but slightly less than, that of the KPD-10 samples. The ultimate relative weight loss for KPD-2 is clearly less than those for the KPD-10 and KPD-5 samples.

Comparing the 5% Ga/silicalite with the KPD-5 sample in Fig. 6, we also note that the HZSM-5 base (3.73% Al_2O_3) promotes significantly more reduction than the silicalite base (0.53% Al_2O_3).

We have also compared reduction rates of KPD-10 samples which have been subjected to both longer (up to 6 h) and shorter ball-milling times. Rates of reduction increase with increasing ball-milling time but the ultimate degree of reduction of KPD-10 is unchanged with ball-milling time. An increase in Ga_2O_3 surface area with increasing ball-milling time probably affects the rate of reduction but a determination of the exact mechanism awaits further kinetic and electron microscopy studies.

C. X-Ray Diffraction

The degree of reduction extracted from the microbalance data would provide all of the information we need to determine a reduction stoichiometry if the reduction process was complete. However, we have found that this is not always the case as

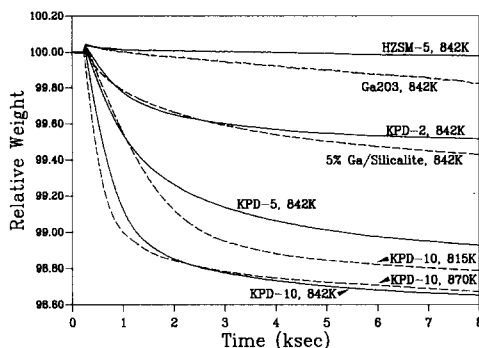


FIG. 6. Isothermal reduction. Specimens dried at 880 K in He prior to introduction of hydrogen.

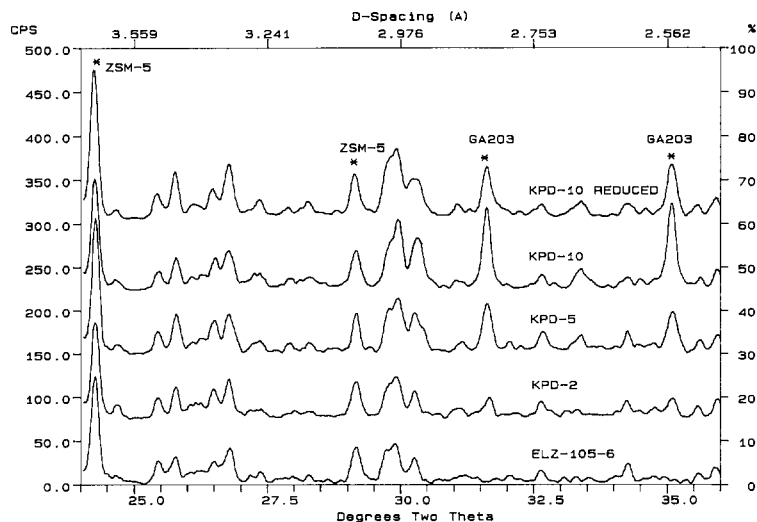


Fig. 7. Demonstration of Ga₂O₃ determination by XRD.

illustrated in Fig. 7, which depicts the 24–36° 2θ region from the XRD. Two HZSM-5 bands at about 24.2° and 29.2° are highlighted in this figure as are two β -Ga₂O₃ lines at about 31.6° and 35.1°. We see that HZSM-5 bands do not interfere with the β -Ga₂O₃ lines and we have therefore used these four bands as a measure of Ga₂O₃ content. Comparing the ELZ-105-6 (HZSM-5) spectrum with the KPD-2, KPD-5, and KPD-10 spectra (which have been derived from catalyst samples which have been ball-milled but not chemically treated), the relative Ga₂O₃ content grows as expected. Thus, we have used the ratio of peak heights as a measure of Ga₂O₃ content and expect the results to be at least semiquantitative. The fifth spectrum in Fig. 7, denoted KPD-10 REDUCED, is a sample taken from an isothermal microbalance reduction experiment at $P_{H_2} = 23$ kPa and 842 K. The relative intensities of the Ga₂O₃ are significantly reduced compared to the KPD-10 lines but are clearly present. Table 2 summarizes the Ga₂O₃ content of a number of different samples taken from the microbalance.

We have also been greatly concerned with the possibility that chemical and thermal treatment of the KPD samples near reaction

conditions promotes substitution of Ga in the HZSM-5 lattice or dealumination. We have therefore computed the Al₂O₃ content by Bibby's method (9) and the unit cell sizes of the ZSM-5 component in a number of samples as in Table 2. A primary problem is that the computed Al₂O₃ content is in general much smaller than the chemical composition given by the manufacturer (3.73%). The reason for this error may be related to XRD resolution in the 45–45.5° region. Von Ballmoos (8) reports six reflections at 45.08°, 45.12°, 45.30°, 45.38°, 45.47°, and 45.54° 2θ in this region. However, when these are encompassed into a real spectrum, lines at 45.08° and 45.12° 2θ appear as a single band while lines at 45.47° and 45.54° 2θ appear as another band with a shoulder due to the less intense 45.30° and 45.38° reflections. The computed profile of von Ballmoos very closely duplicates most of our observed patterns in this region. We have deconvoluted the shoulder band and computed a more exact position for the 45.47/45.54 composite band. This was necessary because some of our spectra showed almost complete resolution of the 45.30/45.38 band from the 45.47/45.54 band and we needed to remove the shoulders in other

TABLE 2

Entry	Reference name	% Ga ₂ O ₃	% Al ₂ O ₃	Cell volume (Å ³)	Notes
Untreated samples					
1	HZSM-5	—	2.62	5372	
2	KPD-2	3.04 ^a	2.57	5372	
3	KPD-5	7.04 ^a	2.75	5364	
4	KPD-10	13.33 ^a	2.61	5368	
5	5% Ga-silicalite	6.30	0.39	5345	
Microbalance samples					
6	HZSM-5/A2	0	2.30	5362	In He, 10 K/min to 1000 K
7	HZSM-5/A8	0	0.92	5345	In He, 10 K/min to 1250 K
8	HZSM-5/A10	0	1.99	5363	In H ₂ , 10 K/min to 950 K
9	HZSM-5/A12	0	2.35	5364	In H ₂ , isothermal, 830 K
10	KPD-2/A1	0.3	2.04	5377	In H ₂ , 10 K/min to 950 K
11	KPD-2/A3	0.0	2.17	5370	In H ₂ , 10 K/min to 900 K
12	KPD-2/A4	—	2.41	—	In H ₂ , isothermal to 830 K
13	KPD-2/A6	0.4	2.47	5377	In H ₂ , isothermal to 830 K
14	KPD-5/A3	0.0	2.14	5367	In H ₂ , 10 K/min, to 900 K
15	KPD-5/A4	0.1	2.50	5371	In H ₂ , 10 K/min, to 900 K
16	KPD-5/A6	2.4	2.72	5382	In H ₂ , isothermal, 830 K
17	KPD-5/A8	5.2	—	5366	In H ₂ , isothermal, 830 K
18	KPD-10/A5	7.0	2.45	5375	In He, 10 K/min to 900 K
19	KPD-10/A6	7.5	2.21	5377	In H ₂ , 10 K/min to 900 K
20	KPD-10/A10	8.9	—	5367	In H ₂ , 10 K/min to 900 K
21	KPD-10/A12	10.2	2.05	5362	In H ₂ , 10 K/min to 900 K ^b
22	KPD-10/A13	6.9	2.16	5361	In H ₂ , 10 K/min to 900 K
23	KPD-10/A14	9.0	2.82	5362	In H ₂ , 3 K/min to 900 K
24	KPD-10/A16	7.6	2.71	5377	In H ₂ , isothermal, 880 K
25	KPD-10/A18	9.3	2.54	5366	In H ₂ , isothermal, 780 K
26	KPD-10/A19	0.6	1.77	5318	In H ₂ , 10 K/min to 1250 K
27	KPD-10/A20	9.2	—	5374	In H ₂ , isothermal 830 K
28	% Ga-silicalite/A2	4.2	1.79	5345	In H ₂ , isothermal, 830 K

^a Used as standards for calibration curve.

^b Ga₂O₃ and HZSM-5 not ball-milled for this sample.

spectra to get consistent positions. Bibby *et al.* (9) do not mention this phenomenon. However, we are really only interested in looking for changes in Al₂O₃ content, and we have considerable evidence that this method does detect changes although there are both consistencies and inconsistencies which we will point out. First, the silicalite sample which is untreated (entry 5, Table 2) displays the correct trend of lower Al₂O₃ content. Second, we were able to detect loss of Al₂O₃ upon heating HZSM-5 samples to 1250 K as in entries 7 and 26, Table 2. HZSM-5 based materials (except for entries

7 and 26) fall pretty well in the 2–2.8% Al₂O₃ range with plenty of scatter but no detectable pattern. We have attempted to correlate these scattered data with unreduced Ga₂O₃ content, the amount of Ga₂O₃ reduced, and unit cell size (which is fairly constant; see next paragraph) without success. We do, however, note a drop in computed Al₂O₃ content from an average of 2.64% for the untreated HZSM-5-based materials (entries 1–4) to an average of 2.35% for HZSM-5-based samples which have not been heated to over 1000 K. This includes a set of samples (entries 6, 8, and 9) which were

not loaded with Ga₂O₃ and therefore this effect, whether real or an anomaly of the method of determination, is probably not due to the Ga₂O₃ loading. Our overall assessment is that we cannot detect an Al₂O₃ content change for the HZSM-5-based materials. The silicalite based catalyst appears to undergo a significant shift from 0.39% for entry 5 (untreated) to 1.79% for entry 28. There is a complication in that Bibby *et al.* (9) report that their Al₂O₃ determination method depends upon the cationic form of the zeolite, and we may be seeing an effect associated with this phenomenon, particularly because this is not accompanied by a change in unit cell size. We will return to this observation later.

We also are not able to detect unit cell size changes during the reduction of KPD catalysts unless the treatment temperature is as high as 1250 K. All unit cell sizes for the HZSM-5 catalysts fall in the range 5361 to 5382 Å³ except for entries 7 and 26 (which have been heated to 1250°K and show a decline in cell size consistent with dealumination) in Table 2. To compare, note the silicalite samples which show a cell size of 5345 Å³ (entries 5 and 28). All of this evidence seems to point to the conclusion that the HZSM-5 crystalline matrix is not altered by Ga₂O₃ loading and reduction.

DISCUSSION

Recently, Gnep and co-workers (6) reported that the activity of mixtures of Ga₂O₃ and HZSM-5 for propane aromatization is much greater than the activity of either pure species. They ascribed this effect to the bifunctional mechanism of the aromatization process and assumed that Ga₂O₃ acts as a dehydrogenation agent, but also noted that they "cannot exclude totally that there are reactions between HZSM-5 and gallium oxide under the operating conditions (high temperature, presence of hydrogen)."

In the present paper, we provide evidence of a strong interaction between Ga₂O₃ and HZSM-5 in the presence of hydrogen even

when the hydrogen is supplied by the propane aromatization reaction. Furthermore, it appears that this interaction leads to the formation of a modified zeolite system which possesses very interesting catalytic properties. Well-known gallium chemistry [for example, see Ref. (10)] suggests that Ga₂O₃ can undergo reduction by H₂ at 873 K to form the suboxide, Ga₂O, which is described as a dark-brown to black amorphous substance which is stable in dry air. We apparently have observed this reduction process directly in TPR-microbalance studies, but at substantially lower temperatures. The reduction evidently involves acidic zeolite lattice sites, first because no reduction took place with pure Ga₂O₃ or Ga₂O₃ on a NaX zeolite substrate, and second because Ga₂O₃/silicalite shows only a very limited reduction of Ga₂O₃. Results of our studies suggest that the intimacy of the Ga₂O₃/HZSM-5 mixing, hydrogen partial pressure, temperature, and temperature programming rate along with the zeolite acidity are all important factors which influence the reduction processes. We do not exclude that there are other factors such as the nature of the reducing agent, or the particular Ga₂O₃ phase (α , β , γ , δ , and ϵ are known and a number of amorphous compounds can still exist), present. Our studies focused on the β -Ga₂O₃ modification which is the most stable modification and probably does not undergo phase transformations prior to reduction. In our opinion, this is a very important point with respect to developing a common theory for the catalytic properties of Ga-containing zeolites, because other popular preparation techniques such as Ga(NO₃)₃ impregnation or ion exchange, or Ga incorporation into the zeolite matrix, may not follow identical phase transformations and reduction pathways especially when different conditions are employed for calcination and reduction.

The degree of reduction of Ga₂O₃ and the weight loss as determined by microbalance can be coupled as follows:

$$\frac{(W_i - W_e)}{MW_{\text{Ga}_2\text{O}_3}} = \frac{\beta}{MW_x}$$

where

$MW_{\text{Ga}_2\text{O}_3} = 188$ g/mole,

MW_x = molecular weight of the volatile component of the reduction product,

β = relative weight loss from the microbalance,

W_i = initial Ga_2O_3 loading in wt%,

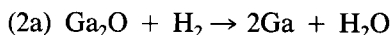
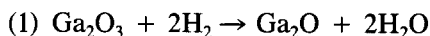
W_e = Ga_2O_3 content at the end of the reduction.

$(W_i - W_e)$ is determined from the x-ray data and β from the microbalance. The unknown in this equation, MW_x , can then be extracted from a plot of β versus $(W_i - W_e)$ which is given in Fig. 8.

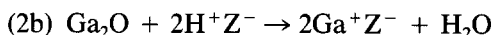
Data in Fig. 8 are clearly scattered primarily as a result of the semiquantitative nature of the determination of $(W_i - W_e)$ by XRD. Also contributing to the scatter is the grouping of the weight loss due to water of hydration and dehydroxylation of HZSM-5 from the weight loss due to reduction. We expect the isothermal weight loss experiments to provide the most accurate data for the determination of β and these points are highlighted in Fig. 8. We should also note that

even for KPD-10 samples which contain in excess of 13 wt% Ga_2O_3 (10 wt% Ga on an elemental basis), we are able to reach only about 6.5 wt% Ga_2O_3 reduced. This suggests that the HZSM-5 is a stoichiometric reactant in the reduction process. We have provided lines representing $MW_x = 32$ and $MW_x = 48$ in Fig. 8. Clearly, MW_x is greater than 32 and $MW_x = 48$ fits the scattered data rather well. This suggests that three water molecules constitute the volatile product of the reduction process (in this estimation, we have noted that the hydrogen in the water molecule is supplied by the gas-phase reactant and therefore will not appear as weight loss from the solid).

With these observations in hand, we suggest the following reduction process:



or



Here H^+Z^- is a proton associated with the anionic zeolite (Z^-). Step 1 follows from known Ga chemistry in that Ga_2O is a product of reduction of Ga_2O_3 with hydrogen. Step 2a is possible to the extent that the XRD/microbalance correlation is correct, but we have no reason to expect that this process would end with a 6.5 wt% Ga_2O_3 limit for KPD-10 samples. We prefer path 2b, which imposes an upper limit on Ga_2O_3 reduction due to the zeolite framework. Since this proposed process requires two protons from the HZSM-5 solid, we would expect $MW_x = 50$ rather than 48, but clearly we are unable to distinguish 50 from 48 statistically with the experimental scatter in Fig. 8. Furthermore, if we perform the stoichiometric analysis using 3.73 wt% Al_2O_3 for the HZSM-5 and assume one proton per Al atom, we compute an upper reduction limit of 6.04% Ga_2O_3 for the KPD-10 catalyst, which agrees quite well with the observed maximum of 6.5% when possible inaccuracies are taken into account. KPD-5 samples can theoretically undergo 6.47% Ga_2O_3 reduction based upon an Al_2O_3 stoi-

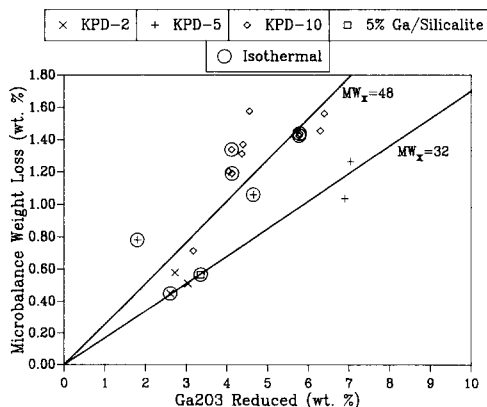


FIG. 8. Correlation of microbalance weight loss with Ga_2O_3 reduction. Circled points represent data that were taken from isothermal reduction experiments.

chiometric limit and we have observed up to 7% reduction.

The 5% Ga/silicalite samples present a problem under this model. We expect a microbalance weight decline of 0.24 wt% if 0.53% Al₂O₃ limits the reduction, but have observed that the silicalite promotes a 0.59 wt% decline. Woolery *et al.* (11) have provided spectroscopic evidence that silicalite contains internal silanols which promote ion exchange independent of framework Al and Chester *et al.* (12) have demonstrated ion-exchange capacity for silicalite in excess of Al content. Endoh *et al.* (13) have proposed that treatment of silicalite with sodium gallate solution results in gallium incorporation into the zeolite lattice at internal silanol sites. We speculate that these silanol groups are responsible for promoting the Ga₂O₃ reduction beyond the known Al₂O₃ content and that the silanol groups provide the protons for step 2b. Since Bibby's method is known to be sensitive to zeolitic cations (9), the change in computed Al₂O₃ content by Bibby's method for the reduced silicalite sample (entry 28 compared to entry 5, Table 2) may be due to the modification of silanol groups by the reduction process and the incorporation of Ga⁺ as a zeolitic cation. The fact that the silicalite base promotes less Ga₂O₃ reduction than a similarly loaded HZSM-5 base is strong evidence in itself that the zeolite is a stoichiometric reactant in the reduction process.

Another possibility is that Ga replaces Al in the zeolite lattice during reduction. However, insertion of Ga for Al should yield a unit cell expansion (14), which has not been observed. Nevertheless, we cannot totally exclude a compensation effect where Al₂O₃ is removed in excess (resulting in a lattice contraction) and that Ga replaces only a portion of the Al₂O₃ (resulting in a compensating lattice expansion). This situation is unlikely in our opinion, especially since we have strong evidence of a 1/1 Ga/Al interaction.

Microbalance and XRD experiments show that the reduction process takes place even at hydrogen partial pressures as low

as 2.5 kPa. However, special discussion is warranted for the observation of increasing selectivity to aromatics with time on stream for catalysts which have not been pre-reduced with H₂ (see Fig. 1). More details of this transient process may be found in a previous publication (15). Under propane reactant flow, we have estimated that the partial pressure of molecular hydrogen due to reaction may not exceed 0.1 kPa. Therefore, the question arises as to whether or not H₂ pressures this low may still promote the reduction process via molecular hydrogen with time scales similar to the observed transient time scale for aromatization enhancement, or whether another reduction mechanism is in operation with a different type of active hydrogen. We have found no reason so far to exclude the possibility that active surface hydrogen produced by an acidic mechanism which may also be involved in hydrogen transfer is involved in the reduction process.

Another interesting feature of our kinetic results is that the time scale for the propane-initiated activation (without H₂ pretreatment) is shorter for higher Ga₂O₃ loadings [Fig. 4; see also Ref. (15)]. This suggests that the activation process is not limited by active or molecular hydrogen but by the transport of Ga species into the zeolite. This is probably a solid-state process rather than one involving the volatilization of Ga species, because an intimate mixture of Ga₂O₃ with HZSM-5 is required before reduction will take place (Fig. 5).

Finally, we focus on the catalytic data which show a dramatic increase in aromatization activity as a result of direct reduction by gas-phase hydrogen. The overall activities and selectivities we have observed are comparable to and even higher than other reports (1-6) where Ga has been introduced by more conventional techniques. Simmons *et al.* (16) have shown that an amorphous gallium oxide phase, which can be produced by steaming gallosilicates, can be linked to *n*-butane cracking activity; Gricus Kofke *et al.* (14) have reported that Ga₂O₃ produced

by calcining ZSM-5 impregnated with $\text{Ga}(\text{NO}_3)_3$ apparently resides outside the zeolite pores. Our findings suggest that these more conventional techniques for Ga loading need to be reexamined with respect to Ga_2O_3 reduction potential and its correlation with catalytic activity.

We also speculate that we have simply created a more efficient route to an active Ga site which offers great potential from a practical point of view, since the method requires no wet operations for the production of a quality catalyst. Further investigations into optimizing the formation of an active catalyst are underway. Investigations designed to elucidate the reaction mechanism and further characterize the active gallium species are still necessary.

ACKNOWLEDGMENTS

V.K. thanks the Bulgarian Academy of Sciences for supporting his visit to the United States. Both authors gratefully acknowledge the financial support from the Exxon Foundation and samples from the Linde Division of Union Carbide.

REFERENCES

1. Mowry, J. R., Anderson, R. F., and Johnson, J. A., *Oil Gas J.*, 128 (1985).
2. Kitagawa, H., Sendoda, Y., and Ono, Y., *J. Catal.* **101**, 12 (1986).
3. Gnep, N. S., Doyemet, J. Y., Seco, A. M., Ramoa Riebeiro, F., and Guisnet, M., *Appl. Catal.* **43**, 105 (1988).
4. Thomas, L. M., and Liu, X., *J. Phys. Chem.* **90**, 4843 (1986).
5. Gnep, N. S., Doyemet, J. Y., and Guisnet, M., *J. Mol. Catal.* **45**, 281 (1988).
6. Gnep, N. S., Doyemet, J. Y., and Guisnet, M., "Zeolites as Catalysts, Sorbents, and Detergent Builders" (Kaye and Weitkamp, Eds.), p. 153. Elsevier, Amsterdam, 1989.
7. Charnell, J. F., *J. Crystal Growth* **8**, 291 (1971).
8. Von Ballmoos, R., "Collection of Simulated XRD Powder Patterns for Zeolites." Butterworths, London, 1984.
9. Bibby, D. M., Aldridge, L. P., and Mileston, N. B., *J. Catal.* **72**, 273 (1981).
10. Sheka, I. A., Chaus, I. S., and Mityureva, T. T., "The Chemistry of Gallium." Elsevier, Amsterdam, 1966.
11. Woolery, G. L., Alemany, L. B., Dessau, R. M., and Chester, A. W., *Zeolites* **6**, 14 (1986).
12. Chester, A. W., Chu, Y. F., Dessau, R. M., and Kresge, C. T., *J. Chem. Soc. Chem. Commun.* **5**, 289 (1985).
13. Endoh, A., Nishimiya, K., Tsutsumi, K., and Takaishi, T., "Zeolites as Catalysts, Sorbents and Detergent Builders" (Karge and Weitkamp, Eds.). Elsevier, Amsterdam, 1989.
14. Gricus Kofke, T. J., Gorte, R. J., and Kokatailo, G. T., *Appl. Catal.* **54**, 177 (1989).
15. Kanazirev, V., Price, G. L., and Dooley, K. M., *J. Chem. Soc. Chem. Commun.*, **9**, 712 (1990).
16. Simmons, D. K., Szostak, R., Agrawal, P. K., and Thomas, T. L., *J. Catal.* **106**, 287 (1987).